Title
mTORC2 mediates CXCL12-induced angiogenesis

Journal
Angiogenesis, 19(3)

ISSN
0969-6970

Authors
Ziegler, Mary E
Hatch, Michaela MS
Wu, Nan
et al.

Publication Date
2016-07-01

DOI
10.1007/s10456-016-9509-6

HHS Public Access

Author manuscript

Angiogenesis. Author manuscript; available in PMC 2017 July 01.

Published in final edited form as:

Angiogenesis. 2016 July ; 19(3): 359–371. doi:10.1007/s10456-016-9509-6.

mTORC2 MEDIATES CXCL12-INDUCED ANGIOGENESIS

Mary E. Ziegler[1], **Michaela M.S. Hatch**[1], **Nan Wu**[1], **Steven A. Muawad**[1], and **Christopher C.W. Hughes**[1,2,3,4]

[1]Department of Molecular Biology and Biochemistry, University of California Irvine, Irvine, CA 92697, USA

[2]Department of Biomedical Engineering, University of California Irvine, Irvine, CA 92697, USA

[3]Edwards Lifesciences Center for Advanced Cardiovascular Technology, University of California Irvine, Irvine, CA 92697, USA

Abstract

The chemokine CXCL12, through its receptor CXCR4, positively regulates angiogenesis by promoting endothelial cell (EC) migration and tube formation. However, the relevant downstream signaling pathways in EC have not been defined. Similarly, the upstream activators of mTORC2 signaling in EC are also poorly defined. Here we demonstrate for the first time that CXCL12 regulation of angiogenesis requires mTORC2 but not mTORC1. We find that CXCR4 signaling activates mTORC2 as indicated by phosphorylation of serine 473 on Akt, and does so through a G-protein- and PI3K-dependent pathway. Significantly, independent disruption of the mTOR complexes by drugs or multiple independent siRNAs reveals that mTORC2, but not mTORC1, is required for microvascular sprouting in a 3D *in vitro* angiogenesis model. Importantly, in a mouse model both tumor angiogenesis and tumor volume are significantly reduced only when mTORC2 is inhibited. Finally, 6-phosphofructo-2-kinase/fructose-2,6-bisphosphatase 3 (PFKFB3), which is a key regulator of glycolytic flux, is required for microvascular sprouting *in vitro*, and its expression is reduced *in vivo* when mTORC2 is targeted. Taken together, these findings identify mTORC2 as a critical signaling nexus downstream of CXCL12/CXCR4 that represents a potential link between mTORC2, metabolic regulation and angiogenesis.

Keywords

CXCL12; CXCR4; angiogenesis; mTOR; Akt; mTORC2

Introduction

Angiogenesis occurs when new blood vessels sprout from existing vasculature and mature into an organized and functional circulatory system [1]. Physiological angiogenesis is

[4]Corresponding Author: Christopher C.W. Hughes Ph.D., University of California, Irvine, Department of Molecular Biology & Biochemistry, 3219 McGaugh Hall Mail Code: 3900, Irvine, CA 92697. Phone: (949) 824-8771, Fax: (949) 824-8551, cchughes@uci.edu.

All applicable international, national, and/or institutional guidelines for the care and use of animals were followed. All procedures performed in studies involving animals were in accordance with the ethical standards of the institution or practice at which the studies were conducted.

stringently regulated and occurs transiently, while pathological angiogenesis, which occurs for example during chronic inflammation or tumor growth, results when positive and negative angiogenic regulators are disrupted [2], and can be persistent. The chemokine CXCL12 (also called SDF-1α) and its receptor CXCR4 are necessary for some, but not all types of angiogenesis [3]. CXCL12 promotes endothelial cell (EC) migration and tube formation and is a stromal cell type-derived factor required for angiogenic sprouting [4,5]. Activation of the CXCL12/CXCR4 signaling axis leads to chemotaxis, cell survival and/or proliferation, however the downstream signaling cascades are tissue specific and not well characterized in EC [6]. Importantly, there is a growing interest in this pathway as a potential "escape route" for tumors that become resistant to anti-VEGF therapy [7].

PI3K is a key downstream regulator of CXCR4-mediated chemotaxis in many cell types, which in turn activates divergent signaling pathways [6]. Mammalian target of rapamycin (mTOR) is an atypical serine/threonine protein kinase that exists in two distinct complexes named mTOR complex 1 (mTORC1) and 2 (mTORC2) and is a key player in PI3K-mediated signal transduction [8]. Both complexes contain the catalytic mTOR subunit, mLST8, DEPTOR and the Tti1/Tel2 complex. mTORC1 is uniquely defined by the proteins raptor and PRAS40, while mTORC2 is identified by the proteins rictor, protor1/2 and mSin1 [8]. mTORC1 responds to growth factors and nutrients and phosphorylates the 4E-BPs and S6Ks [9]. The link between receptor activation and mTORC2 is poorly defined and has even been referred to as "the black box [10]," but it is clear that mTORC2 is responsible for the direct phosphorylation of Akt at S473, SGK1 and PKC-α [10,11]. Both mTOR complexes have been identified as key regulators of cell migration and chemotaxis, but the precise role of each complex in these processes is not fully understood [11].

Evidence for CXCL12 targeting mTOR has come mostly from studies in cancer cells. For example, CXCL12 activates mTOR in human gastric cancer cells and the targeting of mTOR inhibits CXCR4-mediated cell migration [12,13]. In EC, the CXCL12/CXCR4 signaling axis stimulates cell migration and angiogenesis through G-protein-mediated activation of Rac [14]. In cancer cells, a similar pathway leads to mTORC2 activation of Akt and subsequent cell migration [15,16]. Together these findings suggest a potential link between mTORC2 and angiogenic signaling downstream of CXCL12/CXCR4 in EC.

Materials and Methods

Antibodies and inhibitors

The primary antibodies phospho-Akt (S473), phospho-S6RP (S240/244), mTOR, raptor and rictor were all from Cell Signaling. Sin1 was from Millipore, Rheb from Bio-Rad, and β-actin was from LI-COR. The anti-mouse-HRP secondary antibody was from Santa Cruz and the anti-rabbit HRP secondary was from Abcam. The mouse-anti-CD31 used for the *in vivo* studies was from Dianova.

The inhibitors PI-103, PIK-75 and TGX-221 were all from Cayman Chemical. Rapamycin and AMD3100 were from Selleck Chemical and PP242 was from Chemdea. Pertussis toxin was a kind gift from the laboratory of Dr. David Fruman at UCI.

Cell culture conditions and transfection

Primary human umbilical vein endothelial cells (HUVEC) were isolated from umbilical cords obtained from local hospitals under the University of California, Irvine, Institutional Review Board approval and were cultured as previously described [4]. Normal human lung fibroblasts (NHLFs) were purchased from Lonza and cultured in M199 containing 10% FBS. Human cardiac microvascular endothelial cells (HMVECs) were purchased from Lonza and maintained similarly to HUVEC. The BALB/c colon carcinoma cell line CT26.WT (ATCC) was cultured in RPMI (Life Technologies) supplemented with 10% fetal bovine serum.

HUVEC were transfected with siRNA using Lipofectamine 2000 in Opti-MEM (Invitrogen). The sequences of the siRNA to human raptor and rictor (Thermo Scientific) are as follows: Raptor 5′GGGAGAAGCUGGAUUAUUUUU3′ and Rictor 5′GGAAAUAAGGCGAGGUCUAUU3′. siRNA targeting Rheb and Sin1 were ON-TARGETplus siRNA from Thermo Scientific. A non-targeting scrambled control siRNA (Thermo Scientific) was used in all experiments to assess sequence independent effects of siRNA delivery. Transfection efficiency was determined by Western blot (see below).

Western blot analysis

Serum-starved HUVEC were stimulated and/or treated with inhibitors and lysed. Lysates were resolved by SDS-PAGE, and proteins were transferred to Immobilon-P membranes (Millipore). Membranes were blocked in 5% BSA and then incubated overnight with the appropriate antibodies. Primary antibodies to immunoreactive bands were visualized using the appropriate horseradish peroxidase-conjugated antibodies. The Western blot quantification was performed using ImageJ densitometry software.

3D fibrin bead angiogenesis assay

The 3D *in vitro* angiogenesis assay was performed as previously described [17]. Briefly, HUVEC were coated onto Cytodex 3 microcarrier beads (Amersham) and embedded into a fibrin gel (MP Biomedicals). EGM-2 (Lonza) containing NHLFs was added to each well and cultures were maintained for the desired number of days. For quantification, 30 beads were randomly selected in each condition and counted for each experiment. A sprout was only counted if it was at least as long as the diameter of the bead. We also assessed sprout length, but did not find significant differences in any of the conditions tested, and so this parameter is not reported.

3D collagen angiogenesis invasion assay

The 3D collagen invasion assay was performed as previously described [18]. Briefly, HUVEC were seeded on top of rat-tail collagen type I that contained SDF-1 α (400ng/ml) (Peprotech). HUVEC were cultured in serum-free M199 medium containing ITS+3 (Sigma-Aldrich), VEGF (R&D Systems), FGF-2 (R&D Systems), ascorbic acid (Fisher Scientific) and PMA (Calbiochem). For all experiments each condition was plated with 4–5 replicates. EC were allowed to undergo morphogenesis for 24 h. The gels were fixed and stained and the number of invading cells was counted for each condition.

XTT Assay

An XTT assay was performed to determine cell viability. EC were seeded onto 96-well plates and were treated with vehicle control (DMSO), rapamycin (100nM) or PP242 (600nM). After 48 hrs, a standard dilution of EC, which is used to generate the standard curve, were plated onto the 96-well plate and allowed to settle for 3 hrs. The XTT compound (Sigma) was combined with PMS (N-methyl dibenzopyrazine methyl sulfate), the activation agent, and this was added to each well of the plate. The plate was incubated for 2 hrs at 37°C, and then the OD was read at 450nm on a Perkin Elmer Victor^3 plate reader. Viability was determined by comparing the OD obtained from the treated samples to the standard curve. The values are expressed as the percent viability relative to the control.

In vivo Angiogenesis Model

All *in vivo* work was done in accordance with IACUC-approved procedures. Confluent CT26.WT Cells were harvested using 0.5% Trypsin (Life Technologies), and resuspended at 1×10^7 cells/mL. The cells were mixed 1:1 with Matrigel (Corning) to a concentration of 5×10^6 cells/mL. Six-week old BALB/c mice (Charles River) were shaven on the lower left back, just above the hind limb and implanted subcutaneously with 100uL of the Matrigel/cell mix, which contained 500,000 cells. The weight and tumor growth of the mice were monitored daily until the tumor size reached 150mm^3 at which point the mice were sorted into treatment or control groups. Tumor volume was calculated by the formula [(LxW^2)/2]. Control mice were given 200μL of water as the vehicle by intraperitoneal injection. Experimental mice administered either a high or low dosage of rapamycin (1.5mg/kg or 0.5μg/kg, respectively), delivered by intraperitoneal injection. Each group consisted of 7–8 mice. All mice were treated daily for 10 days. At the end of 10 days the mice were euthanized and the tumors were harvested for protein or IHC analysis.

Immunohistochemical Analysis

Tumors were paraffin embedded and sectioned. EC within the tumor sections were visualized by staining for CD31+ cells. Using ImageJ the total percent vascular density of the tumors was calculated by determining the area of CD31+ cells vs the entire area of the section. In addition, the sections were imaged from end to end to obtain the vascular density for each image of the tumor as shown in Figure S7B. Using ImageJ, the degree of vascularization was calculated at a distance of 20%, 40%, 60%, 80% and 100% into the tumor (where 100% was considered the center of the tumor).

Immunofluorescent Analysis

The fixed and paraffin-embedded CT-26 control tumors (described above) were sectioned onto Superfrost +/+ slides. The tumor sections were then rehydrated followed by a heat-activated, sodium citrate antigen retrieval reagent (Vector Labs). The sections were blocked with 1% goat serum (Life Technologies) in PBS for 30 minutes at room temperature and were then incubated with a primary monoclonal rat anti-CD31 antibody (1:20, HistoBioTech) and a primary polyclonal rabbit anti-CXCR4 antibody (1:500, Abcam) diluted in 1% goat serum and 1% BSA overnight at 4°C. The sections were washed several times with PBS and were then incubated for one hour at room temperature with a secondary

goat anti-rabbit 488-conjugated antibody (1:200, Invitrogen) and a secondary goat anti-rat 568-conjugated antibody (1:300, Invitrogen) diluted in 1% goat serum and 1% BSA in PBS. After extensive washing with PBS, the cell nuclei were stained by incubating the sections with DAPI (1μg/mL, Sigma-Aldrich) for 5 minutes at room temperature. The sections were rinsed once with PBS, and each section was mounted with 40μL of ProLong Gold Antifade reagent and a coverslip (Life Technologies). Fluorescent images of the sections were taken using an Olympus IX microscope at 10X and 40X, and the 40X images were analyzed for the co-expression of CXCR4 and CD31.

Statistical Analyses

Researchers were blinded to experimental conditions prior to performing quantifications. All experiments were repeated at least three times with similar results. Data are presented as the mean ± SEM. A Student's t-test was used to analyze the differences between the experimental groups. For comparisons involving three or more conditions and/or two independent time points, a two-way analysis of variance (ANOVA) with multiple comparisons was performed and the TukeyHSD probability value was used to determine significance. Data were consider statistically significant when $p < 0.05$.

Results

The CXCL12/CXCR4 signaling axis is required for sprouting angiogenesis

Previously, in a proteomics analysis of stromal cell-derived factors that contribute to angiogenesis, we showed that pro-angiogenic fibroblasts make CXCL12, and that siRNA-mediated knockdown of CXCL12 expression in fibroblasts significantly inhibited spouting in an *in vitro* angiogenesis assay [4]. In addition, others have identified CXCR4 as a gene enriched in "tip cells" – the EC that lead emerging sprouts [5]. To confirm a role for CXCR4 in mediating the effects of CXCL12 in our system, we used the CXCR4 inhibitor AMD3100. This significantly blocked sprout formation (Figs. 1a and b), confirming the importance of the CXCL12/CXCR4 signaling axis in angiogenic EC.

CXCL12 activates the CXCR4/PI3K/mTORC2 pathway in EC

CXCL12 signal transduction has been defined for a variety of cell types, especially lymphocytes and cancer cells, in which CXCL12 utilizes PI3K to induce Akt phosphorylation. However, little is known about CXCL12 signaling in EC [6]. mTOR is known to be regulated by PI3K [19], and so we hypothesized that CXCL12/CXCR4 activates the mTOR pathway in EC undergoing angiogenic sprouting. To test this, EC were serum starved and stimulated with CXCL12 alone or in combination with the CXCR4 inhibitor AMD3100, or the mTOR inhibitors rapamycin or PP242. The optimal dose and time of CXCL12 stimulation was determined prior to testing the inhibitors (Figs. S1a and b). Signaling through mTORC1 and mTORC2 can be distinguished by Western blot analysis using the downstream targets, S6RP (S240/244) for mTORC1 and Akt (S473) for mTORC2. We found that CXCL12 robustly activated mTORC2 (Fig. 1c), but failed to elevate mTORC1 activity (Fig. S2). Inhibition of CXCR4 with AMD3100, or mTOR with PP242, blocked CXCL12-induced Akt activation (Fig. 1c). To verify that the phosphorylation of Akt occurs through the activation of PI3K in EC, the cells were incubated with specific inhibitors

of PI3K (PIK-75 (p110α) and TGX-221 (p110β)) or a dual PI3K/mTOR inhibitor (PI-103) prior to CXCL12 stimulation. In all cases, PI3K inhibition reduced CXCL12-induced Akt phosphorylation in EC (Fig. 1d). CXCR4 is a G protein-coupled receptor so we next investigated whether CXCL12-induced Akt phosphorylation required G protein activation. Pretreatment with pertussis toxin, a G_i protein inhibitor, abrogated CXCL12-induced Akt phosphorylation at S473, indicating that G_i proteins are required for CXCL12-induced mTORC2 activation in EC (Fig. 1e).

Inhibition of mTORC2 expression by siRNA inhibits angiogenesis in vitro

To further characterize the role of mTOR in angiogenesis, RNAi technology was utilized to knock down raptor and rictor, thereby selectively targeting mTORC1 and mTORC2, respectively. The siRNA targeting raptor downregulated raptor protein expression by ~80%, with no effect on rictor expression, while the rictor siRNA reduced the protein expression of rictor by ~85%, with no effect on raptor expression (Fig. S3). siRNA- transfected ECs were then examined for their ability to undergo angiogenesis *in vitro*. The knockdown of mTORC1 had a very modest effect on EC sprouting; while in contrast, the knockdown mTORC2 strongly inhibited sprouting (Fig. 2a). This phenotype was similar to that seen with blockade of CXCR4 (Figs. 1a and b). To validate these findings we used an additional independent siRNA to both rictor and raptor and obtained identical results (Fig. S4). As a further validation of our findings we disrupted mTOR signal transduction using siRNAs that targeted other proteins important for each complex. mTORC1 signaling was disrupted using an siRNA targeting Rheb, which interacts with mTORC1 to enable its activation [20]. mTORC2 was disrupted by targeting Sin1, which is responsible for maintaining the integrity of mTORC2 [21]. Both Rheb and Sin1 siRNAs reduced target protein expression by approximately 70%, with no effect on the non-target gene (Figs. S5a and b). The knockdown of Rheb (mTORC1) only mildly decreased EC sprouting, whereas Sin1 (mTORC2) knockdown resulted in a highly significant inhibition (Fig. 2b). These data are entirely consistent with the findings obtained by knocking down raptor and rictor. Thus, using multiple independent siRNAs targeting the mTORC2 complex we have confirmed our biochemical data showing that the CXCL12/CXCR4 signaling axis utilizes mTORC2 to stimulate angiogenesis *in vitro*.

Inhibition of mTORC2 activity blocks EC sprouting in vitro

To confirm that mTORC2 activity, in addition to expression, is required for EC sprouting we used rapamycin. Rapamycin is an allosteric inhibitor of mTORC1, but has been shown to also inhibit mTORC2 at higher concentrations [22]. We found that in ECs treated with rapamycin for 24 hrs or more at concentrations at or lower than 0.01pM the phosphorylation of S6RP was significantly reduced, whereas Akt phosphorylation remained unchanged (Fig. S6), which is consistent with inhibition of mTORC1 but not mTORC2. Increasing the concentration of rapamycin to 0.1pM resulted in reduced S6RP and Akt phosphorylation (Fig. S6), which is consistent with inhibiting both mTORC1 and mTORC2. These data established a range of concentrations of rapamycin for which mTORC1 could be selectively targeted in EC. We thus investigated the effects of these concentrations of rapamycin on sprouting (Fig. S6). Rapamycin, at concentrations that only inhibit mTORC1, did not block EC sprouting (Figs. 3a and b). However, when the dose of rapamycin was increased to

0.1pM (a dose at which reductions in mTORC2 signaling can be observed) sprouting was decreased and this reduction was further potentiated at higher doses (Figs. 3a and b). Importantly, we extended these findings to EC from a second source – human cardiac microvessels – where we obtained identical results (Figs. S7a and b). Together, these data demonstrate that mTORC2 is downstream of CXCL12/CXCR4 and is a key regulator of angiogenic sprouting.

mTORC2 is required for CXCL12-induced invasion of EC into collagen gels

Angiogenesis is a multi-step process and a key early step is the migration/invasion of EC into the surrounding extracellular matrix. To specifically assess the role of mTOR in CXCL12-induced EC invasion/migration, a 3D collagen gel invasion assay was performed. In control cultures, we observed robust invasion of ECs (Figs. 4a and b). As expected, cells treated with the CXCR4 inhibitor AMD3100 failed to migrate (Figs. 4a and b). In line with our findings on angiogenic sprouting, mTOR inhibition by rapamycin (at a dose high enough to block both complexes), or by PP242, blocked EC invasion in response to CXCL12 (Figs. 4a and b). In addition, cell viability was assessed in the presence of the mTOR inhibitors at these concentrations and was not significantly different compared to control-treated cells (Fig. S8). To specifically assess the role of each of the mTOR complexes, raptor and rictor were knocked down and the ECs were analyzed for invasive ability. The knockdown of raptor (mTORC1) failed to block CXCL12-induced EC invasion, whereas the knockdown of rictor (mTORC2) significantly reduced EC invasion (Figs 4c and d). These data confirm that mTORC2 signal transduction is necessary for CXCL12-induced invasion/migration.

Inhibition of mTORC2 blocks tumor angiogenesis in vivo

Our data, to this point, demonstrate a critical role for mTORC2 during *in vitro* angiogenesis. To determine the effect of mTOR inhibition on angiogenesis *in vivo,* murine CT26 colon carcinoma cells were mixed with Matrigel and implanted into syngeneic Balb/c mice. Mice were randomized into control or treatment groups once their tumors reached a volume of $150mm^3$. Mice then received either a low or high dose of rapamycin. For each of the drug treatment groups, a matched set of mice was used as the vehicle control. The lower dose of rapamycin was utilized to inhibit only mTORC1, and the higher dose was administered as a comparison to prevent signal transduction through both of the complexes. The tumors were harvested and first analyzed for the co-expression of the EC marker CD31 and CXCR4 in the control tumors by IF. The control tumors demonstrate a high degree of co-expression of these markers, indicating that the ECs within the tumors express CXCR4 and are susceptible to CXCL12 induction (Fig S9). Next, all of the harvested tumors were further analyzed for the expression of CD31 by immunohistochemistry. Control mice showed evidence of a large degree of vessel infiltration into the tumors (Figs. 5a and b). In contrast, mice treated with the higher dose of rapamycin, blocking mTORC1 and mTORC2, showed a significant decrease in CD31+ staining. In sharp contrast, the lower dose of rapamycin, which only blocks mTORC1, failed to significantly decrease vessel density in the tumors (Figs. 5a and b). As an additional measure of vessel infiltration, we analyzed each tumor image in sections to calculate the local vessel density from one side of the tumor to the other, as shown in Figure S10a. For each section of the tumors, there was only a significant decrease in the vessel density in the mice treated with the higher dose of rapamycin (Fig. S10b). To verify

that these doses of rapamycin inhibited mTOR signal transduction as predicted, Western blots were performed using the tumor lysates from a subset of the mice. Mice treated with a low dose of rapamycin showed loss of S6RP (S240/244) phosphorylation (consistent with mTORC1 inhibition) and maintenance of Akt (S473) phosphorylation (consistent with no mTORC2 inhibition). In contrast, mice treated with a higher dose exhibited loss of mTORC1 and mTORC2 signal transduction (Fig. 5c). Tumor volume was also assessed over the course of the drug treatments, and mice treated with a higher dose of rapamycin had a significant decrease in tumor volume compared to the controls. In contrast, tumor volume was not significantly reduced by the lower dose of rapamycin (Fig. 5d). These data support our *in vitro* findings and suggest that angiogenesis in the tumor setting requires mTORC2 signal transduction.

PFKFB3 functions downstream of mTORC2 and is required for angiogenesis

Finally, we wished to investigate potential downstream targets of mTORC2 that might be key regulators of angiogenesis. 6-phosphofructo-2-kinase/fructose-2,6-bisphosphatase 3 (PFKFB3) regulates glycolytic flux and is known to be involved in EC sprouting [23]. We found that PFKFB3 protein expression is reduced in tumor tissue when mice are treated with a higher dose of rapamycin but not the lower dose of rapamycin (Fig. 6a). These data suggest that PFKFB3 is downstream of mTORC2 *in vivo* and that this signaling axis may be required for tumor angiogenesis.

To further explore this concept we utilized both pharmacological inhibition and siRNA targeting of PFKFB3. The PFKFB3 inhibitor 3PO significantly reduced sprouting in a dose-dependent manner (Fig. 6b), and the knockdown of PFKFB3 by siRNA (Fig. S11) significantly reduced EC sprouting in the *in vitro* angiogenesis assay (Fig. 6c). Together, these data identify a link between mTORC2 and PFKFB3 in the regulation of angiogenesis.

Discussion

Tumor-induced angiogenesis results from the activation of a number of signaling pathways in response to angiogenic factors secreted by stromal cells, tumor cells and recruited pro-inflammatory monocytes [24–26]. With the limited success of anti-VEGF therapy in some cancers (e.g. primary colon) there is growing interest in identifying “escape” pathways that might drive angiogenesis [7]. Our data support the idea that the CXCL12/CXCR4 axis may be a pathway worthy of further analysis.

To date there has been a paucity of information on the molecular mechanism of CXCL12/CXCR4 signal transduction in EC as most studies have focused on signal transduction in tumor cells [12,13,6]. mTORC2 is emerging as a central player in the promotion of cell migration via chemotactic receptors [27–29,16], however, the molecular connections linking receptors to mTORC2 activation is poorly understood. Here we propose a model for CXCL12-driven angiogenesis that utilizes mTORC2, but not mTORC1, as a key signaling nexus downstream of CXCR4 (Fig. 7).

When EC are stimulated with CXCL12 the phosphorylation of Akt at S473 is induced, but the phosphorylation of S6RP remains unchanged. This provided us with the initial evidence

that there is a link between the CXCL12/CXCR4 signaling axis and mTORC2. In EC, CXCL12-induced Akt phosphorylation can be blocked with AMD3100, which is a specific CXCR4 inhibitor; thus, supporting the well-established finding that CXCR4 is the major CXC receptor expressed by EC and that CXCL12 is a key chemoattractant for EC [30–33].

CXCL12 can also bind to the receptor CXCR7, but unlike CXCR4, which triggers calcium mobilization and chemotaxis in response to CXCL12, CXCR7 does not efficiently mediate these events [34,35]. Indeed, CXCR7-mediated cellular responses to CXCL12 are not well characterized and it retains its designation as an atypical chemokine receptor [36]. It would be of interest to assess the affect of CXCR7 blockade to determine if this receptor also contributes to CXCL12-induced activation of mTORC2 and the subsequent angiogenic responses in EC, although presumably it would act redundantly.

One of the initial steps leading to the activation of Akt involves PI3K, which via phosphatidylinositol 3,4,5-trisphosphate (PIP3) recruits PDK1 and Akt to the cell membrane [9]. PIP3 has been shown to directly stimulate the kinase activity of mTORC2 [37]. We show that the blockade of PI3K using inhibitors of p110α, p110β or a dual PI3K/mTOR inhibitor reduces CXCL12-induced Akt phosphorylation, with p110α inhibition having a greater effect than p110β inhibition. In addition, pretreatment with pertussis toxin, a G_i protein inhibitor, abolished the activation of Akt at S473 induced by CXCL12. This is in line with reports in T lymphocytes and gastric cancer cells showing that G_i protein is required for CXCL12-induced activation of PI3K and Akt at S473 [12,38]. Taken together these findings provide mechanistic insight into how CXCL12/CXCR4 signals to mTORC2 in EC (Fig. 7).

Previously, mTORC2 was found to form a complex with P-Rex1 [15], a RhoGEF that is critical for cell migration and angiogenesis in response to CXCL12 signaling [14]. These findings suggested a possible connection between mTORC2 and angiogenic signaling downstream of CXCR4. Indeed, we present several lines of evidence that mTORC2 is critical for angiogenesis. Disrupting mTORC2 by knocking down either rictor or Sin1 abrogated angiogenic sprouting to the same degree that blockade of CXCR4 did. In addition, similar disruption of mTORC2 blocked the ability of EC to invade a 3D collagen matrix in response to CXCL12. Finally, we were able to block angiogenic sprouting using a dose of rapamycin that targets both mTORC1 and mTORC2, but could not inhibit sprouting using a dose of rapamycin that only blocks mTORC1 signaling.

In line with our *in vitro* data, inhibiting mTORC1 alone is not sufficient to block tumor angiogenesis or inhibit tumor growth *in vivo*. These processes are only significantly inhibited when mTORC2/Akt is blocked. Several studies have identified prolonged Akt phosphorylation as an important factor contributing to pathological angiogenesis that can be inhibited by higher doses of rapamycin [39,40]; doses that are effective at blocking mTORC2. In addition, our *in vivo* data are supported by evidence from the treatment of renal cell carcinoma, which is a highly vascular neoplasm that is often treated with rapamycin analogs (rapalogs) [41]. The rapalogs improve overall survival or progression-free survival time, which is mediated primarily through the inhibition of mTORC1 [42], but these benefits are only observed in a minority of patients [43]. In fact, the responses are not long lasting and most of the patients experience progression of the disease while on the

treatment [42]. One mechanism proposed to drive this resistance is the lack of mTORC2 inhibition [44]. Thus, the clinical importance of targeting mTORC2 with either prolonged or increased concentrations of rapamycin is now being highlighted [43]. Taken together, the data from both our *in vitro* and our *in vivo* studies identify a novel mechanism that links CXCL12/CXCR4 signaling with angiogenesis through mTORC2.

The next step in understanding the molecular mechanism of how mTORC2 participates in regulating angiogenesis is to examine targets downstream of Akt. mTORC2 fully activates Akt by phosphorylating S473, leading to increased expression of glucose transporters, the phosphorylation and activation of hexokinase 2 to mediate the first step of glycolysis, and the allosteric activation of 6-phosphofructo-1-kinase (PFK-1) [45–47]. During glycolysis, the conversion of fructose-6-phosphate (F6P) to fructose-1,6-bisphosphate ($F1,6P_2$) by PFK-1 is one of the rate-limiting steps of glycolytic flux. 6-phosphofructo-2-kinase/fructose-2,6-biphosphatase 3 (PFKFB3) synthesizes fructose-2,6-bisphosphate ($F2,6P_2$), which is an allosteric activator of PFK-1 and the most potent stimulator of glycolysis [48]. PFKFB3 is activated by Akt [49], and more recently was shown to be a key regulator of angiogenesis [23,50]. Thus, PFKFB3 has been considered a likely candidate for regulation downstream of mTORC2. We confirmed that PFKFB3 was important for angiogenic sprouting *in vitro,* and our data indicate that PFKFB3 expression is reduced *in vivo* when mice are treated with rapamycin at a dose that inhibits both mTORC1 and mTORC2, but not when the dose only blocks mTORC1 signaling, which suggests a potential link between mTORC2 signaling and the regulation of glycolysis through PFKFB3. Future studies will explore this link further.

Until now, the details of downstream CXCL12/CXCR4 signaling in EC, and signaling upstream of mTORC2 in EC have remained elusive. We present a model that unifies these two pathways, with CXCL12/CXCR4 signaling directly activating mTORC2 in EC (Fig. 7). One of the key features of this pathway is that the signal transduction is not occurring through mTORC1. This is important for vascular and cancer biology as we show that to significantly block angiogenesis mTORC2 signaling must be abrogated. This signaling cascade seems to be unique to the EC as tumor cells stimulated with CXCL12 activate both mTOR complexes [12,13,51]. Indeed, recent evidence also shows that EC rely more heavily on the mTORC2 signaling node for VEGF-mediated angiogenesis when compared with mTORC1 [52]. The findings presented here offer the exciting possibility that a chemotactic signal from the tumor microenvironment can trigger mTORC2 activation in EC leading to enhanced angiogenesis. This pathway may therefore contribute to “escape” pathways for tumor EC in patients receiving anti-VEGF therapy.

Supplementary Material

Refer to Web version on PubMed Central for supplementary material.

Acknowledgments

We thank Nazilya Gasanova, Sarah M. Sukardi and Kimberly Lim for their help in quantifying the immunohistochemical specimens, Dr. Kehui Wang of the Pathology Research Services Core at UCI for processing

the tissue sections for analysis and Dr. David Fruman in the Department of Molecular Biology and Biochemistry at UCI for his helpful discussions during the course of these experiments.

This work was supported by the National Institutes of Health/National Cancer Institute Institutional Training Grant Fellowship T32CA009054 to M.E.Z and RO1 HL60067 to C.C.W.H. The content is solely the responsibility of the authors and does not necessarily represent the official views of the National Cancer Institute or the National Institutes of Health. C.C.W.H. receives support from the Chao Family Comprehensive Cancer Center through a National Cancer Institute Center Grant, P30A062203.

References

1. Weis SM, Cheresh DA. Tumor angiogenesis: molecular pathways and therapeutic targets. Nat Med. 2011; 17(11):1359–1370. nm.2537 [pii]. DOI: 10.1038/nm.2537 [PubMed: 22064426]
2. Carmeliet P, Jain RK. Molecular mechanisms and clinical applications of angiogenesis. Nature. 2011; 473(7347):298–307. nature10144 [pii]. DOI: 10.1038/nature10144 [PubMed: 21593862]
3. Salcedo R, Oppenheim JJ. Role of chemokines in angiogenesis: CXCL12/SDF-1 and CXCR4 interaction, a key regulator of endothelial cell responses. Microcirculation. 2003; 10(3–4):359–370. 7800200 [pii]. DOI: 10.1038/sj.mn.7800200 [PubMed: 12851652]
4. Newman AC, Chou W, Welch-Reardon KM, Fong AH, Popson SA, Phan DT, Sandoval DR, Nguyen DP, Gershon PD, Hughes CC. Analysis of stromal cell secretomes reveals a critical role for stromal cell-derived hepatocyte growth factor and fibronectin in angiogenesis. Arterioscler Thromb Vasc Biol. 2013; 33(3):513–522. ATVBAHA.112.300782 [pii]. DOI: 10.1161/ATVBAHA.112.300782 [PubMed: 23288153]
5. Strasser GA, Kaminker JS, Tessier-Lavigne M. Microarray analysis of retinal endothelial tip cells identifies CXCR4 as a mediator of tip cell morphology and branching. Blood. 2010; 115(24):5102–5110. blood-2009-07-230284 [pii]. DOI: 10.1182/blood-2009-07-230284 [PubMed: 20154215]
6. Teicher BA, Fricker SP. CXCL12 (SDF-1)/CXCR4 pathway in cancer. Clin Cancer Res. 2010; 16(11):2927–2931. 1078-0432.CCR-09-2329 [pii]. DOI: 10.1158/1078-0432.CCR-09-2329 [PubMed: 20484021]
7. Duda DG, Kozin SV, Kirkpatrick ND, Xu L, Fukumura D, Jain RK. CXCL12 (SDF1alpha)-CXCR4/CXCR7 pathway inhibition: an emerging sensitizer for anticancer therapies? Clin Cancer Res. 2011; 17(8):2074–2080. 1078-0432.CCR-10-2636 [pii]. DOI: 10.1158/1078-0432.CCR-10-2636 [PubMed: 21349998]
8. Laplante M, Sabatini DM. mTOR signaling in growth control and disease. Cell. 2012; 149(2):274–293. S0092-8674(12)00351-0 [pii]. DOI: 10.1016/j.cell.2012.03.017 [PubMed: 22500797]
9. Bracho-Valdes I, Moreno-Alvarez P, Valencia-Martinez I, Robles-Molina E, Chavez-Vargas L, Vazquez-Prado J. mTORC1- and mTORC2-interacting proteins keep their multifunctional partners focused. IUBMB Life. 2011; 63(10):896–914. DOI: 10.1002/iub.558 [PubMed: 21905202]
10. Laplante M, Sabatini DM. mTOR signaling at a glance. J Cell Sci. 2009; 122(Pt 20):3589–3594. 122/20/3589 [pii]. DOI: 10.1242/jcs.051011 [PubMed: 19812304]
11. Liu L, Parent CA. Review series: TOR kinase complexes and cell migration. J Cell Biol. 2011; 194(6):815–824. jcb.201102090 [pii]. DOI: 10.1083/jcb.201102090 [PubMed: 21930774]
12. Chen G, Chen SM, Wang X, Ding XF, Ding J, Meng LH. Inhibition of chemokine (CXC motif) ligand 12/chemokine (CXC motif) receptor 4 axis (CXCL12/CXCR4)-mediated cell migration by targeting mammalian target of rapamycin (mTOR) pathway in human gastric carcinoma cells. J Biol Chem. 2012; 287(15):12132–12141. M111.302299 [pii]. DOI: 10.1074/jbc.M111.302299 [PubMed: 22337890]
13. Hashimoto I, Koizumi K, Tatematsu M, Minami T, Cho S, Takeno N, Nakashima A, Sakurai H, Saito S, Tsukada K, Saiki I. Blocking on the CXCR4/mTOR signalling pathway induces the anti-metastatic properties and autophagic cell death in peritoneal disseminated gastric cancer cells. Eur J Cancer. 2008; 44(7):1022–1029. S0959-8049(08)00134-2 [pii]. DOI: 10.1016/j.ejca.2008.02.043 [PubMed: 18375114]
14. Carretero-Ortega J, Walsh CT, Hernandez-Garcia R, Reyes-Cruz G, Brown JH, Vazquez-Prado J. Phosphatidylinositol 3,4,5-triphosphate-dependent Rac exchanger 1 (P-Rex-1), a guanine nucleotide exchange factor for Rac, mediates angiogenic responses to stromal cell-derived factor-1/chemokine stromal cell derived factor-1 (SDF-1/CXCL-12) linked to Rac activation,

endothelial cell migration, and in vitro angiogenesis. Mol Pharmacol. 2010; 77(3):435–442. mol.109.060400 [pii]. DOI: 10.1124/mol.109.060400 [PubMed: 20018810]

15. Hernandez-Negrete I, Carretero-Ortega J, Rosenfeldt H, Hernandez-Garcia R, Calderon-Salinas JV, Reyes-Cruz G, Gutkind JS, Vazquez-Prado J. P-Rex1 links mammalian target of rapamycin signaling to Rac activation and cell migration. J Biol Chem. 2007; 282(32):23708–23715. M703771200 [pii]. DOI: 10.1074/jbc.M703771200 [PubMed: 17565979]
16. Kim EK, Yun SJ, Ha JM, Kim YW, Jin IH, Yun J, Shin HK, Song SH, Kim JH, Lee JS, Kim CD, Bae SS. Selective activation of Akt1 by mammalian target of rapamycin complex 2 regulates cancer cell migration, invasion, and metastasis. Oncogene. 2011; 30(26):2954–2963. onc201122 [pii]. DOI: 10.1038/onc.2011.22 [PubMed: 21339740]
17. Nakatsu MN, Hughes CC. An optimized three-dimensional in vitro model for the analysis of angiogenesis. Methods Enzymol. 2008; 443:65–82. S0076-6879(08)02004-1 [pii]. DOI: 10.1016/S0076-6879(08)02004-1 [PubMed: 18772011]
18. Koh W, Stratman AN, Sacharidou A, Davis GE. In vitro three dimensional collagen matrix models of endothelial lumen formation during vasculogenesis and angiogenesis. Methods Enzymol. 2008; 443:83–101. S0076-6879(08)02005-3 [pii]. DOI: 10.1016/S0076-6879(08)02005-3 [PubMed: 18772012]
19. Hemmings BA, Restuccia DF. PI3K-PKB/Akt pathway. Cold Spring Harb Perspect Biol. 2012; 4(9):a011189. 4/9/a011189 [pii]. doi: 10.1101/cshperspect.a011189 [PubMed: 22952397]
20. Long X, Lin Y, Ortiz-Vega S, Yonezawa K, Avruch J. Rheb binds and regulates the mTOR kinase. Curr Biol. 2005; 15(8):702–713. S0960-9822(05)00226-5 [pii]. DOI: 10.1016/j.cub.2005.02.053 [PubMed: 15854902]
21. Jacinto E, Facchinetti V, Liu D, Soto N, Wei S, Jung SY, Huang Q, Qin J, Su B. SIN1/MIP1 maintains rictor-mTOR complex integrity and regulates Akt phosphorylation and substrate specificity. Cell. 2006; 127(1):125–137. S0092-8674(06)01147-0 [pii]. DOI: 10.1016/j.cell.2006.08.033 [PubMed: 16962653]
22. Sarbassov DD, Ali SM, Sengupta S, Sheen JH, Hsu PP, Bagley AF, Markhard AL, Sabatini DM. Prolonged rapamycin treatment inhibits mTORC2 assembly and Akt/PKB. Mol Cell. 2006; 22(2):159–168. S1097-2765(06)00218-8 [pii]. DOI: 10.1016/j.molcel.2006.03.029 [PubMed: 16603397]
23. De Bock K, Georgiadou M, Schoors S, Kuchnio A, Wong BW, Cantelmo AR, Quaegebeur A, Ghesquiere B, Cauwenberghs S, Eelen G, Phng LK, Betz I, Tembuyser B, Brepoels K, Welti J, Geudens I, Segura I, Cruys B, Bifari F, Decimo I, Blanco R, Wyns S, Vangindertael J, Rocha S, Collins RT, Munck S, Daelemans D, Imamura H, Devlieger R, Rider M, Van Veldhoven PP, Schuit F, Bartrons R, Hofkens J, Fraisl P, Telang S, Deberardinis RJ, Schoonjans L, Vinckier S, Chesney J, Gerhardt H, Dewerchin M, Carmeliet P. Role of PFKFB3-driven glycolysis in vessel sprouting. Cell. 2013; 154(3):651–663. S0092-8674(13)00776-9 [pii]. DOI: 10.1016/j.cell.2013.06.037 [PubMed: 23911327]
24. Ferrara N, Gerber HP, LeCouter J. The biology of VEGF and its receptors. Nat Med. 2003; 9(6):669–676. nm0603-669 [pii]. DOI: 10.1038/nm0603-669 [PubMed: 12778165]
25. Mazzieri R, Pucci F, Moi D, Zonari E, Ranghetti A, Berti A, Politi LS, Gentner B, Brown JL, Naldini L, De Palma M. Targeting the ANG2/TIE2 axis inhibits tumor growth and metastasis by impairing angiogenesis and disabling rebounds of proangiogenic myeloid cells. Cancer Cell. 2011; 19(4):512–526. S1535-6108(11)00081-X [pii]. DOI: 10.1016/j.ccr.2011.02.005 [PubMed: 21481792]
26. Orimo A, Gupta PB, Sgroi DC, Arenzana-Seisdedos F, Delaunay T, Naeem R, Carey VJ, Richardson AL, Weinberg RA. Stromal fibroblasts present in invasive human breast carcinomas promote tumor growth and angiogenesis through elevated SDF-1/CXCL12 secretion. Cell. 2005; 121(3):335–348. S0092-8674(05)00237-0 [pii]. DOI: 10.1016/j.cell.2005.02.034 [PubMed: 15882617]
27. Zhang F, Zhang X, Li M, Chen P, Zhang B, Guo H, Cao W, Wei X, Cao X, Hao X, Zhang N. mTOR complex component Rictor interacts with PKCzeta and regulates cancer cell metastasis. Cancer Res. 2010; 70(22):9360–9370. 0008-5472.CAN-10-0207 [pii]. DOI: 10.1158/0008-5472.CAN-10-0207 [PubMed: 20978191]
28. Kuehn HS, Jung MY, Beaven MA, Metcalfe DD, Gilfillan AM. Prostaglandin E2 activates and utilizes mTORC2 as a central signaling locus for the regulation of mast cell chemotaxis and

mediator release. J Biol Chem. 2011; 286(1):391–402. M110.164772 [pii]. DOI: 10.1074/jbc.M110.164772 [PubMed: 20980255]

29. Liu L, Das S, Losert W, Parent CA. mTORC2 regulates neutrophil chemotaxis in a cAMP- and RhoA-dependent fashion. Dev Cell. 2010; 19(6):845–857. S1534-5807(10)00531-9 [pii]. DOI: 10.1016/j.devcel.2010.11.004 [PubMed: 21145500]
30. Feil C, Augustin HG. Endothelial cells differentially express functional CXC-chemokine receptor-4 (CXCR-4/fusin) under the control of autocrine activity and exogenous cytokines. Biochem Biophys Res Commun. 1998; 247(1):38–45. S0006-291X(98)98499-6 [pii]. DOI: 10.1006/bbrc.1998.8499 [PubMed: 9636650]
31. Gupta SK, Lysko PG, Pillarisetti K, Ohlstein E, Stadel JM. Chemokine receptors in human endothelial cells. Functional expression of CXCR4 and its transcriptional regulation by inflammatory cytokines. J Biol Chem. 1998; 273(7):4282–4287. [PubMed: 9461627]
32. Salcedo R, Wasserman K, Young HA, Grimm MC, Howard OM, Anver MR, Kleinman HK, Murphy WJ, Oppenheim JJ. Vascular endothelial growth factor and basic fibroblast growth factor induce expression of CXCR4 on human endothelial cells: In vivo neovascularization induced by stromal-derived factor-1alpha. Am J Pathol. 1999; 154(4):1125–1135. S0002-9440(10)65365-5 [pii]. [PubMed: 10233851]
33. Volin MV, Joseph L, Shockley MS, Davies PF. Chemokine receptor CXCR4 expression in endothelium. Biochem Biophys Res Commun. 1998; 242(1):46–53. S0006-291X(97)97890-6 [pii]. DOI: 10.1006/bbrc.1997.7890 [PubMed: 9439607]
34. Burns JM, Summers BC, Wang Y, Melikian A, Berahovich R, Miao Z, Penfold ME, Sunshine MJ, Littman DR, Kuo CJ, Wei K, McMaster BE, Wright K, Howard MC, Schall TJ. A novel chemokine receptor for SDF-1 and I-TAC involved in cell survival, cell adhesion, and tumor development. J Exp Med. 2006; 203(9):2201–2213. jem.20052144 [pii]. DOI: 10.1084/jem.20052144 [PubMed: 16940167]
35. Zabel BA, Wang Y, Lewen S, Berahovich RD, Penfold ME, Zhang P, Powers J, Summers BC, Miao Z, Zhao B, Jalili A, Janowska-Wieczorek A, Jaen JC, Schall TJ. Elucidation of CXCR7-mediated signaling events and inhibition of CXCR4-mediated tumor cell transendothelial migration by CXCR7 ligands. J Immunol. 2009; 183(5):3204–3211. jimmunol.0900269 [pii]. DOI: 10.4049/jimmunol.0900269 [PubMed: 19641136]
36. Naumann U, Cameroni E, Pruenster M, Mahabaleshwar H, Raz E, Zerwes HG, Rot A, Thelen M. CXCR7 functions as a scavenger for CXCL12 and CXCL11. PLoS One. 2010; 5(2):e9175.doi: 10.1371/journal.pone.0009175 [PubMed: 20161793]
37. Gan X, Wang J, Su B, Wu D. Evidence for direct activation of mTORC2 kinase activity by phosphatidylinositol 3,4,5-trisphosphate. J Biol Chem. 2011; 286(13):10998–11002. M110.195016 [pii]. DOI: 10.1074/jbc.M110.195016 [PubMed: 21310961]
38. Sotsios Y, Whittaker GC, Westwick J, Ward SG. The CXC chemokine stromal cell-derived factor activates a Gi-coupled phosphoinositide 3-kinase in T lymphocytes. J Immunol. 1999; 163(11):5954–5963. ji_v163n11p5954 [pii]. [PubMed: 10570282]
39. Guba M, von Breitenbuch P, Steinbauer M, Koehl G, Flegel S, Hornung M, Bruns CJ, Zuelke C, Farkas S, Anthuber M, Jauch KW, Geissler EK. Rapamycin inhibits primary and metastatic tumor growth by antiangiogenesis: involvement of vascular endothelial growth factor. Nat Med. 2002; 8(2):128–135. nm0202-128 [pii]. DOI: 10.1038/nm0202-128 [PubMed: 11821896]
40. Phung TL, Ziv K, Dabydeen D, Eyiah-Mensah G, Riveros M, Perruzzi C, Sun J, Monahan-Earley RA, Shiojima I, Nagy JA, Lin MI, Walsh K, Dvorak AM, Briscoe DM, Neeman M, Sessa WC, Dvorak HF, Benjamin LE. Pathological angiogenesis is induced by sustained Akt signaling and inhibited by rapamycin. Cancer Cell. 2006; 10(2):159–170. S1535-6108(06)00216-9 [pii]. DOI: 10.1016/j.ccr.2006.07.003 [PubMed: 16904613]
41. Sharma SG, Nanda S, Longo S. Anti-angiogenic therapy in renal cell carcinoma. Recent Pat Anticancer Drug Discov. 2010; 5(1):77–83. PRA-ABS-Sharma-10 [pii]. [PubMed: 19601920]
42. Battelli C, Cho DC. mTOR inhibitors in renal cell carcinoma. Therapy. 2011; 8(4):359–367. DOI: 10.2217/thy.11.32 [PubMed: 21894244]
43. Kornakiewicz A, Solarek W, Bielecka ZF, Lian F, Szczylik C, Czarnecka AM. Mammalian Target of Rapamycin Inhibitors Resistance Mechanisms in Clear Cell Renal Cell Carcinoma. Curr Signal

Transduct Ther. 2014; 8(3):210–218. CSTT-8-210 [pii]. DOI: 10.2174/1574362409666140206222746 [PubMed: 25152703]

44. Choo AY, Yoon SO, Kim SG, Roux PP, Blenis J. Rapamycin differentially inhibits S6Ks and 4E-BP1 to mediate cell-type-specific repression of mRNA translation. Proc Natl Acad Sci U S A. 2008; 105(45):17414–17419. 0809136105 [pii]. DOI: 10.1073/pnas.0809136105 [PubMed: 18955708]
45. Deprez J, Vertommen D, Alessi DR, Hue L, Rider MH. Phosphorylation and activation of heart 6-phosphofructo-2-kinase by protein kinase B and other protein kinases of the insulin signaling cascades. J Biol Chem. 1997; 272(28):17269–17275. [PubMed: 9211863]
46. Gottlob K, Majewski N, Kennedy S, Kandel E, Robey RB, Hay N. Inhibition of early apoptotic events by Akt/PKB is dependent on the first committed step of glycolysis and mitochondrial hexokinase. Genes Dev. 2001; 15(11):1406–1418. DOI: 10.1101/gad.889901 [PubMed: 11390360]
47. Kohn AD, Summers SA, Birnbaum MJ, Roth RA. Expression of a constitutively active Akt Ser/Thr kinase in 3T3-L1 adipocytes stimulates glucose uptake and glucose transporter 4 translocation. J Biol Chem. 1996; 271(49):31372–31378. [PubMed: 8940145]
48. Van Schaftingen E, Hue L, Hers HG. Fructose 2,6-bisphosphate, the probably structure of the glucose- and glucagon-sensitive stimulator of phosphofructokinase. Biochem J. 1980; 192(3):897–901. [PubMed: 6453589]
49. Manes NP, El-Maghrabi MR. The kinase activity of human brain 6-phosphofructo-2-kinase/fructose-2,6-bisphosphatase is regulated via inhibition by phosphoenolpyruvate. Arch Biochem Biophys. 2005; 438(2):125–136. S0003-9861(05)00161-X [pii]. DOI: 10.1016/j.abb.2005.04.011 [PubMed: 15896703]
50. Xu Y, An X, Guo X, Habtetsion TG, Wang Y, Xu X, Kandala S, Li Q, Li H, Zhang C, Caldwell RB, Fulton DJ, Su Y, Hoda MN, Zhou G, Wu C, Huo Y. Endothelial PFKFB3 plays a critical role in angiogenesis. Arterioscler Thromb Vasc Biol. 2014; 34(6):1231–1239. ATVBAHA.113.303041 [pii]. DOI: 10.1161/ATVBAHA.113.303041 [PubMed: 24700124]
51. Monterrubio M, Mellado M, Carrera AC, Rodriguez-Frade JM. PI3Kgamma activation by CXCL12 regulates tumor cell adhesion and invasion. Biochem Biophys Res Commun. 2009; 388(2):199–204. S0006-291X(09)01496-X [pii]. DOI: 10.1016/j.bbrc.2009.07.153 [PubMed: 19660434]
52. Wang S, Amato KR, Song W, Youngblood V, Lee K, Boothby M, Brantley-Sieders DM, Chen J. Regulation of Endothelial Cell Proliferation and Vascular Assembly through Distinct mTORC2 Signaling Pathways. Mol Cell Biol. 2015; MCB.00306-14 [pii]. doi: 10.1128/MCB.00306-14

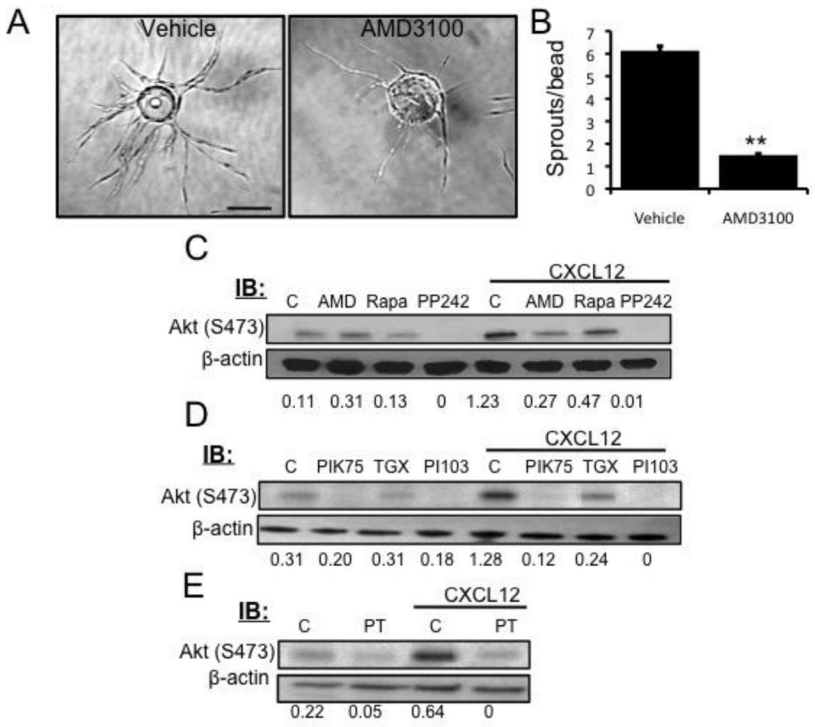

Fig. 1.

CXCL12/CXCR4 activation regulates angiogenesis by triggering mTORC2

(**a**) EC were coated onto Cytodex beads and embedded in a fibrin gel. NHLFs were seeded on top of the gel, and twenty-four hours after embedding AMD3100 (1μM) was added to the medium. DMSO was used as a vehicle control and fresh inhibitor was added with each medium change. Beads were fixed at day 7 and imaged. Scale bar: 150 μm. (**b**) The number of sprouts per bead was quantified. (**c**–**e**) Serum-starved EC were stimulated with CXCL12 (50 ng/ml, 30 min) alone or after pretreatment with AMD3100 (1μM, 1 hr), rapamycin (100 nM, 24 hr), PP242 (600 nM, 24hr), PIK-75 (500 nM, 1 hr), TGX-221 (500 nM, 1 hr), PI-103 (250 nM, 1hr) or Pertussis Toxin (100ng/mL, 2 hr). DMSO was used as a vehicle control. The level of Akt phosphorylation (S473) was determined by Western blot. β-actin was used as a loading control. The phospho-bands was measured and normalized using ImageJ. The numbers below the blots indicate the level of phospho-Akt relative to the lowest expression (n = 3).

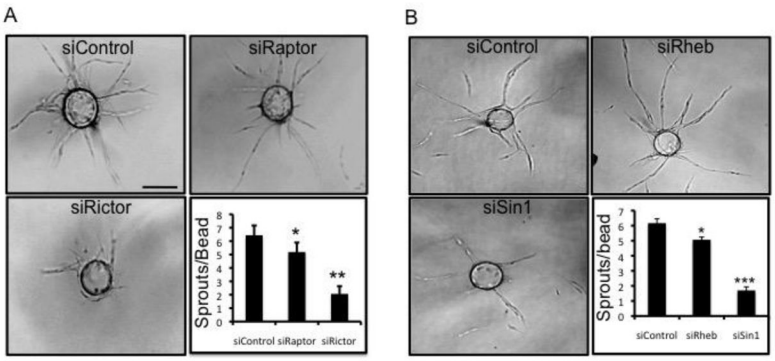

Fig. 2.

mTORC2 is required for sprouting angiogenesis

(**a**) EC were transfected with control, raptor or rictor siRNA or (**b**) with control, Sin1 or Rheb siRNA. Twenty-four hours later a fibrin sprouting assay (as described above) was performed. The beads were fixed at day 7 and imaged. Scale bar: 150 μm. The number of sprouts per bead was quantified. The error bars represent the SEM (*$p < 0.05$; **$p < 0.01$). All experiments were repeated a minimum of 3 times with similar results.

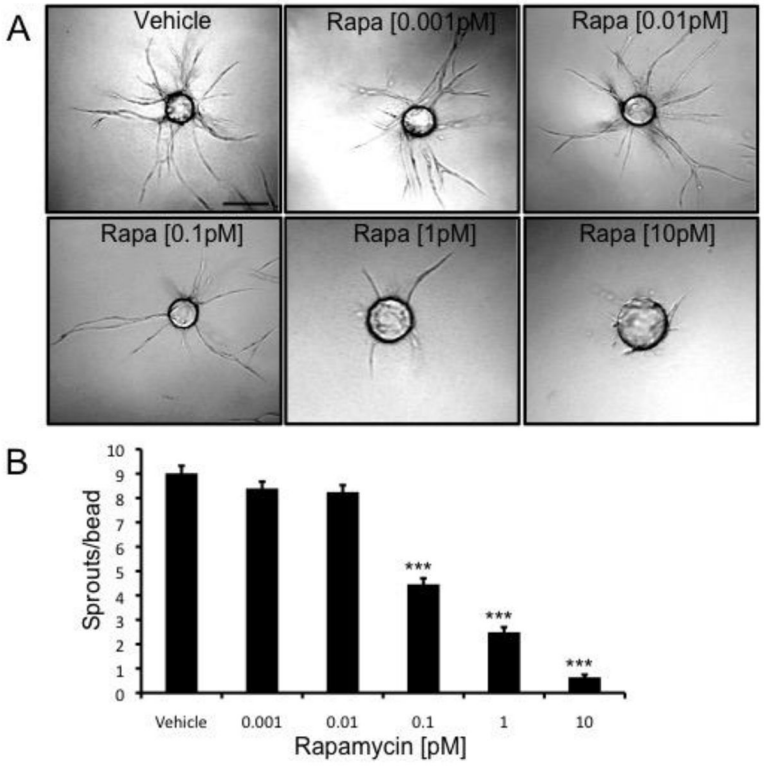

Fig. 3.

Inhibiting mTORC2 signaling blocks angiogenic sprouting

(**a**) A fibrin bead sprouting assay was performed as described in Figure 1 and twenty-four hours after embedding the cells were treated with rapamycin as indicated, with DMSO used as a vehicle control. The inhibitor was replaced with each medium change and the beads were fixed at day 7 for imaging. Scale bar: 150 μm. (**b**) The number of sprouts per bead was quantified. The error bars represent the SEM (***$p < 0.001$). The experiment was repeated a minimum of 3 times with similar results.

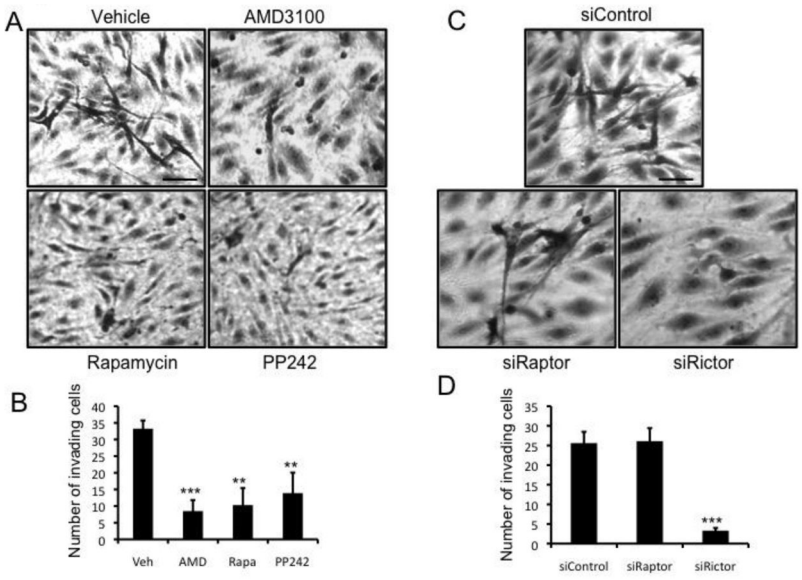

Fig. 4.

CXCL12-induced EC invasion is dependent on mTORC2

(**a**) EC were seeded onto collagen gels containing CXCL12 and incubated with vehicle (DMSO) control or AMD3100 (1μM), rapamycin (100nM) or PP242 (600nM) for 24 hrs after before fixing and imaging. Scale bar: 150 μm. (**b**) The average number of invading cells was calculated by counting 5 wells per condition. (**c**) ECs were transfected with either control, raptor or rictor siRNA. Forty-eight hours after transfection the cells were seeded onto collagen gels containing CXCL12 and incubated for 24 hrs after which time the gels were fixed and imaged. Scale bar: 150 μm. (**d**) The average number of invading cells was calculated by counting 5 wells per condition. The error bars represent the SEM (**$p < 0.01$; ***$p < 0.001$). All experiments were repeated a minimum of 3 times with similar results.

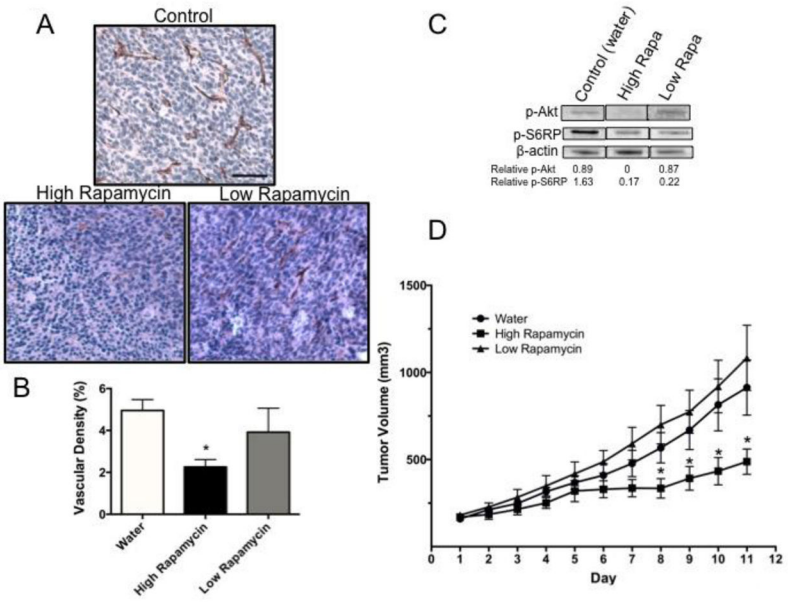

Fig. 5.

mTORC2 inhibition suppresses tumor angiogenesis *in vivo*

(**a**) BALB/c mice were implanted subcutaneously with CT26 tumor cells. Once the tumor reached a volume of 150mm^3 the mice were administered either a high or low dose of rapamycin (1.5mg/kg or 0.5μg/kg, respectively) or water as a control, delivered by intraperitoneal injection. Each group consisted of 5–6 mice and all mice were treated daily for 10 days. Tumors were paraffin embedded and sectioned and EC within the tumor sections were visualized by staining for CD31+ cells. Scale Bar: 150 μm. (**b**) The vascular density in the tumors was calculated using ImageJ by determining the area of CD31+ cells relative to the entire area of the section. (**c**) Tumor tissue from the mice was collected and homogenized in lysis buffer. The tissue lysates were run on an SDS-PAGE gel and a Western blot was performed. The membranes were probed for phoshpo-Akt (S473) and phospho-S6-RP (S240/244) and β-actin was used as a loading control. Bands were quantified using ImageJ and the expression of phospho-protein relative to the control mice is indicated below the blot. The images are all from the same blot and separated to present only the relevant treatment groups. (**d**) Tumor volume was monitored daily. Error bars represent the SEM *p < 0.05.

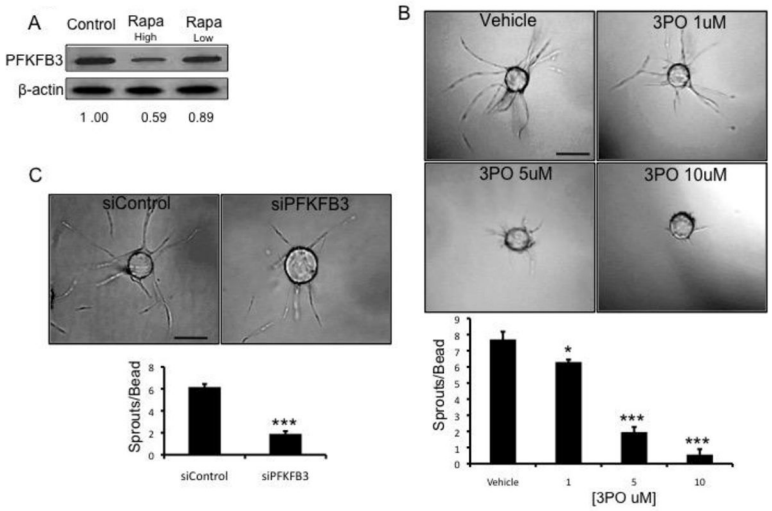

Fig. 6.

mTORC2 inhibition decreases the expression of PFKFB3. (**a**) Tumor tissue from the mice described in Figure 5 was collected and homogenized in lysis buffer and PFKFB3 expression was analyzed by Western blot. β-actin was used as a loading control. Bands were quantified using ImageJ and intensities are indicated below the blot as PFKFB3 expression relative to the control mice. (**b**) A fibrin bead angiogenesis assay was performed as described above and twenty-four hours after embedding the cells were treated with 3PO as indicated. DMSO was used as a vehicle control and the inhibitor was replaced with each medium change. The beads were fixed at day 7 and the number of sprouts per bead was quantified. Scale bar: 150 μm. (**c**) EC were transfected with either control or PFKFB3 siRNA and twenty-four hours later a fibrin bead angiogenic assay was performed. The beads were fixed at day 7 and imaged. Scale bar: 150 μm. The number of sprouts per bead was quantified. The error bars represent the SEM (**p < 0.01; ***p < 0.001). All experiments were repeated a minimum of 3 times with similar results.

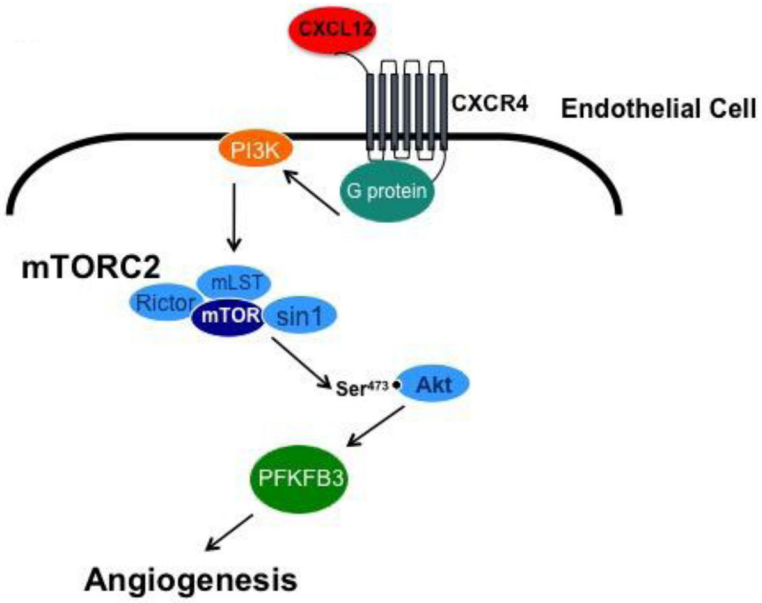

Fig. 7.

CXCL12/CXCR4 signal transduction in EC is mTORC2 dependent

The activation of CXCR4 on EC by CXCL12 initiates G protein signaling leading to PI3K activation, which then triggers mTORC2 to phosphorylate Akt at S473. CXCL12 stimulation does not potentiate signal transduction downstream of mTOR1. The disruption or inhibition of mTORC2 blocks angiogenesis both *in vitro* and *in vivo*. Inhibition of mTORC2 *in vivo* reduces the expression of PFKFB3 placing this metabolic regulator downstream of the mTORC2 signaling cascade and designates these targets as key regulators of angiogenesis.